Journal of Materials Chemistry C

PAPER

View Article Online
View Journal

Published on 22 December 2014. Downloaded by Universidade de Lisboa on 29/01/2015 11:20:32.

Cite this: DOI: 10.1039/c4tc02833c

Room temperature ferromagnetism in $(Ga_{1-x}Mn_x)_2O_3$ epitaxial thin films

Daoyou Guo,[ab] Zhenping Wu,[ab] Yuehua An,[ab] Xiaojiang Li,[e] Xuncai Guo,[ab] Xulong Chu,[ab] Changlong Sun,[ab] Ming Lei,[ab] Linghong Li,[f] Lixin Cao,[d] Peigang Li*[ac] and Weihua Tang*[ab]

Received 10th December 2014
Accepted 22nd December 2014

DOI: 10.1039/c4tc02833c

www.rsc.org/MaterialsC

Mn-doped monoclinic β-$(Ga_{1-x}Mn_x)_2O_3$ thin films were epitaxially grown on α-Al_2O_3 (0001) substrates by alternately depositing Ga_2O_3 and Mn layers using the laser molecular beam epitaxy technique. The crystal lattice expands and the energy band gap shrinks with the increase of Mn content for Mn ions incorporated into the Ga site. Ferromagnetism appears even above room temperature when $x \geq 0.11$ and can be remarkably enhanced with the continuous increase of Mn indicated by the increased magnetization and coercivity. This study presents a promising candidate for use in spintronic devices that are capable of working at room temperature.

Introduction

Magnetic semiconductors have attracted considerable attention due to their potential applications in spintronic devices,[1–5] such as fast nonvolatile semiconductor memories and integrated magnetic/electronic/photonic devices. According to the theoretical prediction by Dietl,[6] a high Curie temperature (T_c) even exceeding room temperature could be achieved in some wide band gap semiconductors when they are doped with transition metals, especially Mn. The thus-far doping work has been carried out mainly in some conventional II–VI and III–V compounds,[7–12] such as (Ga, Mn)As, (In, Mn)As, (Ga, Mn)N, (Zn, Mn)O, *etc.*, while the mechanism for the appearance of ferromagnetism remains rather elusive. The discovery of more ferromagnetic semiconductors is always desired not only because they can provide complementary knowledge helpful for clarifying the fundamental issue but also due to their potential practical applications. Gallium oxide (Ga_2O_3), a wide direct band gap semiconductor with a gap size of ~4.9 eV,[13–15] is a good place for such exploration. High photon energy and high transparency in the visible and ultraviolet regions (>280 nm) enable easy manipulation of the spins by photons, and thus make Ga_2O_3 attractive for use in spintronic devices.

Ga_2O_3 can crystallize in five different phases (known as α, β, γ, δ, and ε-phases).[16] Among these, the monoclinic β-Ga_2O_3 (space group: $C2/m$) with the lattice parameters of $a = 12.23$ Å, $b = 3.04$ Å, $c = 5.80$ Å, and $\beta = 103.7°$ has been recognized as the most stable phase suitable for various characterizations and more intensively studied.[16–18] Ferromagnetism was observed in Mn-doped γ-Ga_2O_3 at room temperature as well as in a highly crystalline corundum-structured α-$(Ga_{1-x}Fe_x)_2O_3$ ($x = 0.58$) thin film.[19–21] However, magnetic properties of Mn-doped β-Ga_2O_3 have not been studied yet. In this work, we report on the observation of ferromagnetism even above room temperature in epitaxially grown Mn-doped β-Ga_2O_3 thin films with high Mn concentrations.

Experimental

The film growth of Mn-doped β-Ga_2O_3 was performed by using the laser molecular beam epitaxy technique with a pulse energy density of ~5 J cm^{-2} on α-Al_2O_3 (0001) substrates at 900 °C. The Ga_2O_3 and Mn layers were alternately deposited and both depositions were repeated 20 times. The Mn concentrations were controlled by solely changing the laser pulse numbers during each run of depositing the Mn layers (defined as N, $N =$ 10, 20, 30, 40, 50) while those for depositing Ga_2O_3 layers in each run were fixed at 100. The alternating deposition enabled the realization of $(Ga_{1-x}Mn_x)_2O_3$ thin films with different compositions due to interdiffusion between Mn and Ga_2O_3 layers at high temperature. The Mn concentrations in $(Ga_{1-x}Mn_x)_2O_3$ films were determined to be 6.06 at%, 10.97 at%, 17.64 at%, 31.17 at%, and 53.10 at% respectively by X-ray energy dispersive spectroscopy (EDS). The orientation and crystallinity

[a]School of Science, Beijing University of Posts and Telecommunications, Beijing 100876, China. E-mail: whtang@bupt.edu.cn
[b]State Key Laboratory of Information Photonics and Optical Communications, Beijing University of Posts and Telecommunications, Beijing 100876, China
[c]Center for Optoelectronics Materials and Devices, Department of Physics, Zhejiang Sci-Tech University, Hangzhou 310018, Zhejiang, China. E-mail: pgli@zstu.edu.cn
[d]Beijing National Laboratory for Condensed Matter Physics, Institute of Physics, Chinese Academy of Science, Beijing 100190, China
[e]State Key Laboratory of Functional Materials for Informatics, Shanghai Institute of Microsystem and Information Technology, Chinese Academy of Sciences, Shanghai 200050, China
[f]Department of Physics, The State University of New York at Potsdam, Potsdam, New York 13676-2294, USA

Published on 22 December 2014. Downloaded by Universidade de Lisboa on 29/01/2015 11:20:32.

of the as-grown films were investigated by X-ray diffraction (XRD) at θ–2θ scan and *in situ* reflection high-energy electron diffraction (RHEED). The valences of Mn ions and element distribution were analyzed by X-ray photoelectron spectroscopy (XPS) and secondary ion mass spectrometry (SIMS). Magnetic properties of the films were measured using a commercial superconducting quantum interference device (SQUID), Quantum design.

Results and discussion

The crystal structures of the as-grown films were characterized from θ–2θ scans of XRD; the results are shown in Fig. 1(a). Except diffraction peaks of the Al_2O_3 substrate, only diffraction peaks located at around 19°, 38°, and 59° were observed, all of them belong to $(Ga_{1-x}Mn_x)_2O_3$. No peaks from Mn metal clusters, Mn oxide, Mn_xGa_y or $MnGa_2O_4$ phases existed. As seen from the enlarged view of θ–2θ XRD patterns around 38° (Fig. 1(b)), the peaks are located at 38.34°, 38.12°, 37.94°, 37.77°, 37.60°, and 37.15° for $x = 0$, 0.06, 0.11, 0.18, 0.31, and 0.53, respectively, indicating that the peak gradually shifts to smaller 2θ with the increase of x. Meanwhile, no abrupt shift or half height width changes of diffraction peak were observed with the increase of x (the relatively large shift for $x = 0.53$ may be attributed to the relatively much increase of Mn content from 0.31 to 0.53). Thus, the possibility of phase transformation would be excluded. According to relevant references, the $(\bar{2}01)$ diffraction peak of β-Ga_2O_3 (PDF#43-1012) and the (222) diffraction peak of γ-Ga_2O_3 (ref. 19 and 20) should be located at 38.40° and 37.28°, respectively. For $x = 0.06$, if γ-phase appears, the diffraction peak around 38° should present an abrupt shift to near, even lower than 37.28° due to Mn doping. Actually, the peak locates at 38.12° which is closer to 38.40° of the β-phase. Thus, we believe that β-Ga_2O_3 is obtained by Mn-doping. The diffraction peaks located at around 19°, 38°, and 59° correspond to $(\bar{2}01)$ and higher order peaks of monoclinic β-phase Ga_2O_3 respectively, indicating a preferred $(\bar{2}01)$ plane orientation of the thin films. The x dependence of the $(\bar{2}01)$ plane distance is depicted in Fig. 1(c), showing that the d spacing increases almost linearly with the increase of x. With the increase of x, the peak shift of the $(\bar{2}01)$ plane to smaller 2θ indicates a gradual increase of the lattice constants because the radii of Mn ions are larger than that of the Ga ion (Mn^{2+}, Mn^{3+} and Ga^{3+} ionic radii are 0.83, 0.64 and 0.62 Å, respectively).[22,23] These facts, along with the EDS results, demonstrate the successful incorporation of Mn ions into the lattice of Ga_2O_3. The clear and streaky RHEED patterns shown in Fig. 1(d) suggest that the $(Ga_{1-x}Mn_x)_2O_3$ films are of single phase with very smooth surfaces.

Hayashi *et al.* reported that the Mn-doped Ga_2O_3 (7 cation% of Mn) thin film grown at 500° exhibits the spinel structure of the γ-phase.[19] According to the temperature dependent phase transformation by Roy,[16] the γ-phase is metastable and would transfer to the stable monoclinic β-phase above 650 °C. It is reasonable for Mn-doped Ga_2O_3 thin films exhibiting the γ-phase when the films are deposited at 500 °C. When the deposition temperature is above 600 °C, β-Ga_2O_3 will appear in Mn-doped Ga_2O_3 films,[24] indicating that the transformation of the γ-phase to β-phase has begun at 600 °C. Herein, the $(Ga_{1-x}Mn_x)_2O_3$ thin films were grown at a substrate temperature of 900 °C, all the metastable phases would transfer to β phases. We have characterized the $(Ga_{1-x}Mn_x)_2O_3$ thin film with $x = 0.06$ using selected-area electron diffraction patterns in an orientation parallel to $(10\bar{1}0)$ of the Al_2O_3 substrate, and the results confirmed that the obtained film was β-Ga_2O_3.[20] More sophisticated research is underway.

Compositions as a function of film thickness were also characterized by using the SIMS depth profiling. The results for the representative $(Ga_{0.47}Mn_{0.53})_2O_3$ film are summarized in Fig. 2 by showing intensities of the Mn and Ga ion currents as a function of sputter depth of the film. Intensities of both Mn and Ga ion currents remain almost constant indicating that Mn is

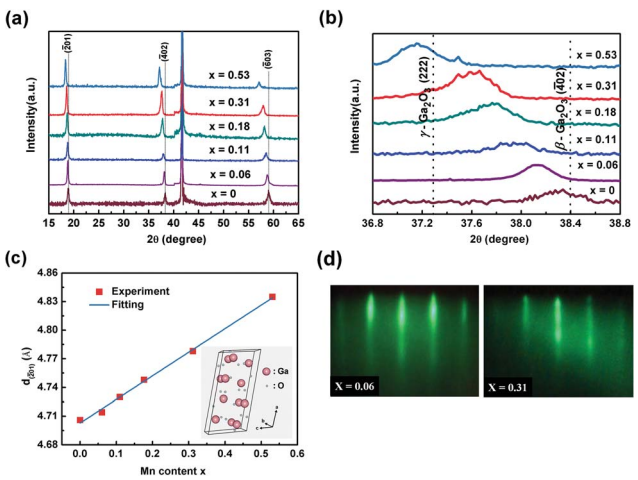

Fig. 1 (a) θ–2θ XRD patterns, (b) enlarged view of θ–2θ XRD patterns around 38°, (c) the Mn doping concentration dependence of the $(\bar{2}01)$ lattice plane distance, and (d) RHEED patterns of $(Ga_{1-x}Mn_x)_2O_3$ thin films ($x = 0.06$, 0.31).

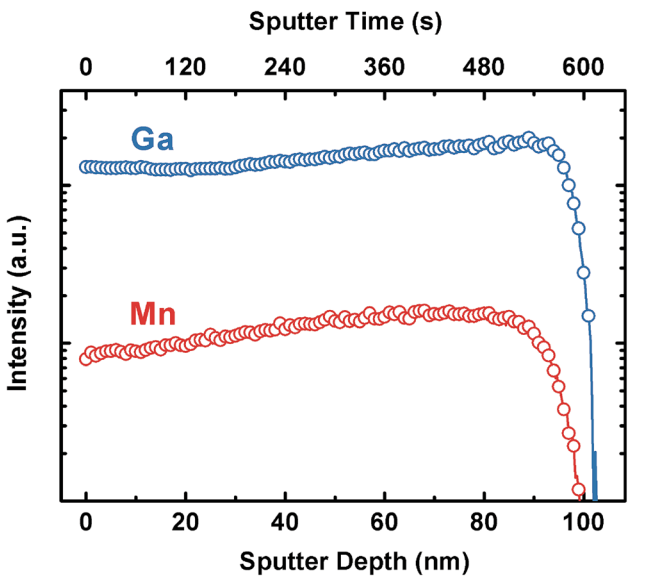

Fig. 2 Mn and Ga SIMS depth profiles for the $(Ga_{0.47}Mn_{0.53})_2O_3$ thin film.

This journal is © The Royal Society of Chemistry 2015

Published on 22 December 2014. Downloaded by Universidade de Lisboa on 29/01/2015 11:20:32.

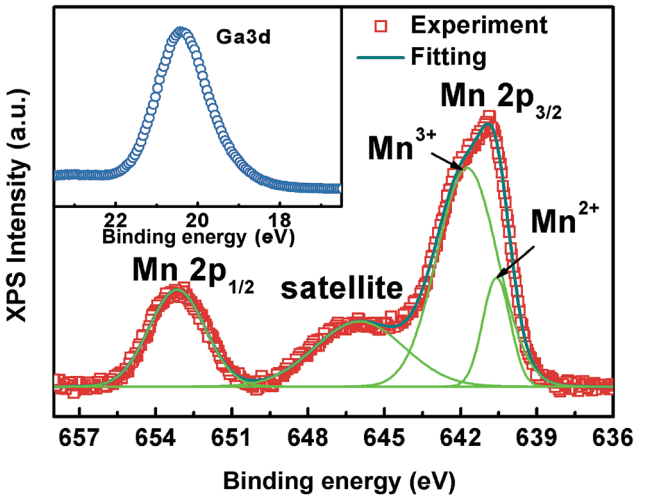

Fig. 3 XPS spectra of Mn 2p and Ga 3d (inset) core levels for the $(Ga_{0.47}Mn_{0.53})_2O_3$ thin film.

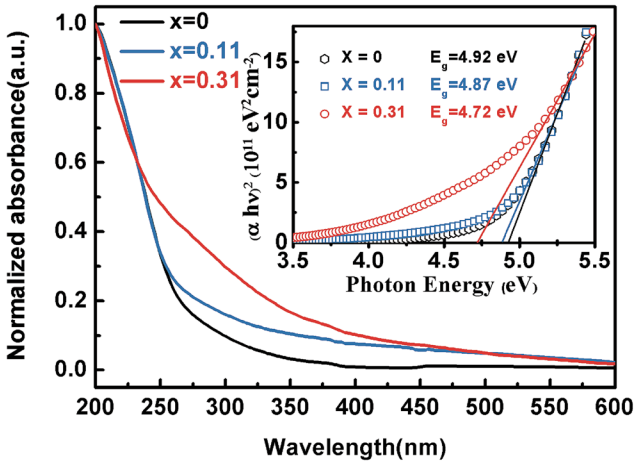

Fig. 4 Absorption spectra of $(Ga_{1-x}Mn_x)_2O_3$ ($x = 0.11$, 0.31) thin films compared with that of a pure β-Ga_2O_3 thin film and the plot of $(\alpha h\nu)^2$ *versus* $h\nu$ (inset).

actually uniformly distributed in the film without any detectable enrichment or segregation. Meanwhile, the streak lines of RHEED patterns always remain sharp during the growth processes, indicating that Mn ions are uniformly distributed in-plane. These results thus evidently exclude the possibility of formation of Mn-rich layers in $(Ga_{1-x}Mn_x)_2O_3$ thin films.

The chemical compositions and chemical states of Mn ions in the films were characterized by using XPS, as presented in Fig. 3. The elements present in the $(Ga_{0.47}Mn_{0.53})_2O_3$ film are Mn, Ga, O, and C (not shown). The charge-shift spectrum was calibrated using the fortuitous C 1s peak at 284.8 eV. The spectrum of Mn 2p shows a spin–orbit doublet ($j = 3/2$, 1/2). The Mn $2p_{3/2}$ main peak has a satellite structure on the higher binding-energy side separated by ~6 eV, which indicates a strong Coulomb interaction between the Mn 3d electrons and hybridization between the Mn 3d and other valence orbitals.[25] No Mn $2p_{3/2}$ peaks for metallic Mn (located at 639 eV) are visible in Fig. 3, indicating no Mn metallic clusters present in the films.[26] It is also noted that the Mn $2p_{3/2}$ main peak contains two peaks corresponding to 640.59 and 641.74 eV, respectively, implying the presence of two possible valence states (Mn^{2+}/Mn^{3+}) with a ratio of about 19 : 81. The neutral configuration of Mn in Ga_2O_3 should be Mn^{3+} when viewed as replacing Ga^{3+} in the lattice. However, there are many oxygen vacancies as donor-type defects in β-Ga_2O_3 thin films, which would lead to the valence of Mn change from +3 to +2.[14] In addition, as seen from the XPS spectrum of the Ga 3d core-level in the inset of Fig. 3, there is only one peak at 20.4 eV, which comes from the Ga ions in the $(Ga_{1-x}Mn_x)_2O_3$ films.[27] And another peak at ~18.4 eV for decomposed Ga atoms cannot be found,[27] suggesting that the metallic Ga or Mn_xGa_y is not present in our samples.

The band gap of $(Ga_{1-x}Mn_x)_2O_3$ thin films can be modified by changing the Mn content, indicated by the ultraviolet-visible (UV-Vis) absorbance measurements. Shown by the absorbance spectra of $(Ga_{1-x}Mn_x)_2O_3$ ($x = 0$, 0.11, 0.31) thin films in Fig. 4, the spectrum of the host exhibits a sharp intrinsic absorption edge at ~250 nm,[28] whilst those of Mn-doped samples display clear red-shift. The gap sizes can be derived by fitting the linear region of the $(\alpha h\nu)^2$ *versus* $h\nu$ plot, shown by the inset in Fig. 4. The gap size decreases from 4.92 eV for $x = 0$ to 4.87 eV and 4.72 eV for $x = 0.11$ and $x = 0.31$, respectively.

Fig. 5 shows the magnetization *versus* magnetic field (M–H) curves of $(Ga_{1-x}Mn_x)_2O_3$ films at room temperature measured with the applied magnetic field parallel to the films. The diamagnetic contribution from the sapphire substrate was subtracted from the data. The $(Ga_{0.94}Mn_{0.06})_2O_3$ film displays typical paramagnetic behavior while $(Ga_{1-x}Mn_x)_2O_3$ thin films with $x \geq 0.11$ show hysteresis loops indicative of ferromagnetism. However, for γ-phase Mn-doped Ga_2O_3, the film with a Mn concentration even of 7% has shown room temperature ferromagnetism with a magnetization of 2.8 emu cm^{-3} at 2 kOe,[19] which may be attributed to different phase types of $(Ga_{1-x}Mn_x)_2O_3$ thin films. Magnetic parameters for $(Ga_{1-x}Mn_x)_2O_3$

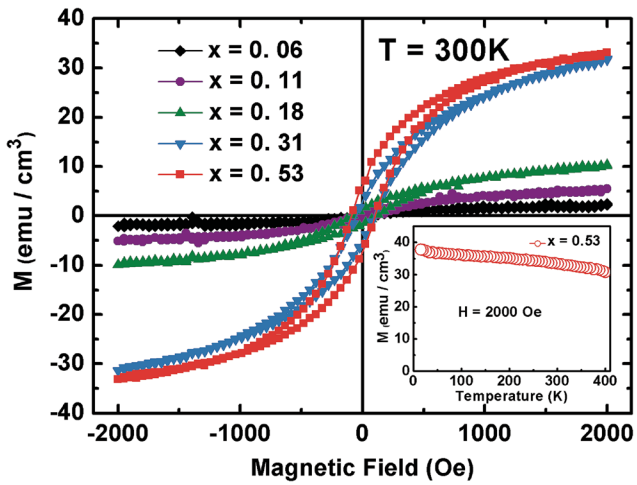

Fig. 5 M–H curves of $(Ga_{1-x}Mn_x)_2O_3$ thin films at room temperature and temperature dependent magnetization of the $(Ga_{0.47}Mn_{0.53})_2O_3$ thin film at 2 kOe (inset).

Published on 22 December 2014. Downloaded by Universidade de Lisboa on 29/01/2015 11:20:32.

Table 1 Magnetic parameters for $(Ga_{1-x}Mn_x)_2O_3$ thin films with different Mn contents. The given M_s values are at a magnetic field of 2 kOe

Mn content (x)	M_s (emu cm^{-3})	Coercivity (Oe)	M_r (emu cm^{-3})
0.1097	5.5	62	0.8
0.1764	10.4	80	1.6
0.3117	31.6	98	5.4
0.5310	33.1	109	7.6

films with respect to x are listed in Table 1. The saturation magnetizations (M_s) increase monotonically from 5.5 emu cm^{-3} to the maximum value of 33.1 emu cm^{-3} at 2 kOe with the increase of x and the coercivity and magnetic remanence (M_r) increase as well, revealing apparent enhancement of ferromagnetism with the increase of Mn content. For the $(Ga_{0.47}Mn_{0.53})_2O_3$ film, the coercivity and M_r reach ~109 Oe and 7.6 emu cm^{-3}, respectively. The temperature dependent magnetization (M–T) of the $(Ga_{0.47}Mn_{0.53})_2O_3$ film was measured at 2 kOe in field-cooling mode. As seen from the M–T curve shown in the inset of Fig. 5, M is seen to be fairly constant in the measurement temperature range of 15–400 K.

The above XRD, SIMS, XPS, UV-Vis absorption, and magnetic property characterizations on $(Ga_{1-x}Mn_x)_2O_3$ films are sufficient to confirm the successful substitution of Mn for Ga. Meanwhile, according to the XRD and XPS analyses, we did not find any ferromagnetic second phase, such as Mn_xGa_y clusters. Nevertheless, for the possible secondary phases of Mn metal and Mn-based oxides, only Mn_3O_4 is ferromagnetic with a small T_c of 43 K while others are all antiferromagnetic.[10,29] It is reasonable to conclude that the room temperature ferromagnetism in the $(Ga_{1-x}Mn_x)_2O_3$ thin films with high Mn concentrations is intrinsic.

Until now, there has been no perfect model that can well describe the origin of the room-temperature ferromagnetism of Mn-doped Ga_2O_3. Hayashi *et al.*[19] suggested that the room temperature ferromagnetism of γ-$(Ga_{1-x}Mn_x)_2O_3$ can be explained by a carrier-mediated double exchange model that had been used to explain room temperature ferromagnetism in Mn-doped GaN. Pei *et al.*[30] also used the model to propose the ferromagnetic coupling in their theoretical study on magnetic properties of Mn-doped β-Ga_2O_3 and pointed out that the ferromagnetic ground state could be established even at a small Mn concentration of 12.5 at%. For the carrier-mediated double exchange model, a large quantity of mobile carriers are desired to induce ferromagnetism.[4,31] However, in our system, the charge carriers should be highly localized due to the high intrinsic properties of β-Ga_2O_3 hosts, as a result, we failed to measure the carrier type and carrier concentration in $(Ga_{1-x}Mn_x)_2O_3$ thin films using Hall effect measurement. So the framework of the bound magnetic polaron (BMP) model should be more suitable. In the BMP model, ferromagnetic exchange is mediated through localized donor electrons in the impurity band.[32] The interactions of BMPs in an insulator follow essentially from the Loss and DiVincenzo[33] proposal for spin-based solid-state quantum computing electrons localized in electrostatically defined quantum dots, with coupling between electron spins *via* the exchange interaction. Based on the doping level, the ferromagnetism coupling could be classified into three main processes in the BMP model.[34,35] In minor doping, the remote impurities produce low magnetic moments for weak interaction. In appropriate doping, a sufficiently large number of bound magnetic polarons' long-range ferromagnetic order would be established. While in heavy doping, the increase of dopant concentration will strengthen dopant–dopant associations and lead to progressive orbital moment quenching, causing the decrease of the ferromagnetism. The BMP model seems to be more suitable for our experiment results, but it does not mean that the BMP is a satisfactory model to explain room-temperature ferromagnetism in $(Ga_{1-x}Mn_x)_2O_3$. In order to deeper understand the mechanism, more experimental and theoretical work should be done to improve the current models or propose a better model.

Conclusions

In conclusion, monoclinic $(Ga_{1-x}Mn_x)_2O_3$ thin films with a preferable $(\bar{2}01)$ orientation on α-Al_2O_3 (0001) substrates were epitaxially grown by using the laser molecular beam epitaxy technique. The systematic characterizations by XRD, SIMS, XPS and UV-Vis absorbance spectra confirmed the incorporation of Mn into the lattice of β-Ga_2O_3 and revealed its effects on the crystal and electronic structures. Magnetic property measurements revealed that the $(Ga_{1-x}Mn_x)_2O_3$ thin films are ferromagnetic even above room temperature, and the ferromagnetism can be enhanced by increasing the Mn content.

Acknowledgements

This work was supported by the National Natural Science Foundation of China (no. 61274017, 51172208, 11404029), Fund of State Key Laboratory of Information Photonics and Optical Communications (BUPT), the Beijing University of Posts and Telecommunications (BUPT) Excellent Ph.D. Students Foundation (no. CX201421), China Postdoctoral Science Foundation Funded Project (Grant no. 2014M550661), the Fundamental Research Funds for the Central Universities (Grant no. 2014RC0906), Beijing Natural Science Foundation (2154055), and National Basic Research Program of China (973 Program) (2010CB923202).

References

1 S. Wolf, D. Awschalom, R. Buhrman, J. Daughton, S. Von Molnar, M. Roukes, A. Y. Chtchelkanova and D. Treger, *Science*, 2001, **294**, 1488.
2 L. Chen, L. Guo, Z. Li, H. Zhang, J. Lin, J. Huang, S. Jin and X. Chen, *Sci. Rep.*, 2013, **3**, 2599.
3 S. Fusil, V. Garcia, A. Barthélémy and M. Bibes, *Annu. Rev. Mater. Res.*, 2014, **44**, 91.
4 X. Lia and J. Yang, *J. Mater. Chem. C*, 2014, **2**, 7071.
5 Y. Liu, G. Wang, S. Wang, J. Yang, L. Chen, X. Qin, B. Song, B. Wang and X. Chen, *Phys. Rev. Lett.*, 2011, **106**, 087205.

 This journal is © The Royal Society of Chemistry 2015

Published on 22 December 2014. Downloaded by Universidade de Lisboa on 29/01/2015 11:20:32.

6 T. Dietl, H. Ohno, F. Matsukura, J. Cibert and D. Ferrand, *Science*, 2000, **287**, 1019.
7 A. MacDonald, P. Schiffer and N. Samarth, *Nat. Mater.*, 2005, **4**, 195.
8 Y. Liu, L. Jiang, G. Wang, S. Zuo, W. Wang and X. Chen, *Appl. Phys. Lett.*, 2012, **100**, 122401.
9 N. Theodoropoulou, A. Hebard, M. Overberg, C. Abernathy, S. Pearton, S. Chu and R. Wilson, *Phys. Rev. Lett.*, 2002, **89**, 107203.
10 S. Jung, S. J. An, G. C. Yi, C. Jung, S. I. Lee and S. Cho, *Appl. Phys. Lett.*, 2002, **80**, 4561.
11 S. Sonoda, I. Tanaka, F. Oba, H. Ikeno, H. Hayashi, T. Yamamoto, Y. Yuba, Y. Akasaka, K. Yoshida, M. Aoki, M. Asari, T. Araki, Y. Nanishi, K. Kindo and H. Hori, *Appl. Phys. Lett.*, 2007, **90**, 012504.
12 B. Song, K. Zhu, J. Liu, J. Jian, J. Han, H. Bao, H. Li, Y. Liu, H. Zuo, W. Wang, G. Wang, X. Zhang, S. Meng, W. Wang and X. Chen, *J. Mater. Chem.*, 2010, **20**, 9935.
13 W. Feng, X. Wang, J. Zhang, L. Wang, W. Zheng, P. Hu, W. Cao and B. Yang, *J. Mater. Chem. C*, 2014, **2**, 3254.
14 D. Y. Guo, Z. P. Wu, Y. H. An, X. C. Guo, X. L. Chu, C. L. Sun, L. H. Li, P. G. Li and W. H. Tang, *Appl. Phys. Lett.*, 2014, **105**, 023507.
15 T. Oshima, T. Okuno, N. Arai, N. Suzuki, S. Ohira and S. Fujita, *Appl. Phys. Express*, 2008, **1**, 011202.
16 R. Roy, V. Hill and E. Osborn, *J. Am. Chem. Soc.*, 1952, **74**, 719.
17 K. Matsuzaki, H. Yanagi, T. Kamiya, H. Hiramatsu, K. Nomura, M. Hirano and H. Hosono, *Appl. Phys. Lett.*, 2006, **88**, 092106.
18 K. Matsuzaki, H. Hiramatsu, K. Nomura, H. Yanagi, T. Kamiya, M. Hirano and H. Hosono, *Thin Solid Films*, 2006, **496**, 37.
19 H. Hayashi, R. Huang, H. Ikeno, F. Oba, S. Yoshioka, I. Tanaka and S. Sonoda, *Appl. Phys. Lett.*, 2006, **89**, 181903.
20 R. Huang, H. Hayashi, F. Oba and I. Tanaka, *J. Appl. Phys.*, 2007, **101**, 063526.
21 K. Kaneko, I. Kakeya, S. Komori and S. Fujita, *J. Appl. Phys.*, 2013, **113**, 233901.
22 Y. An, S. Wang, L. Duan, J. Liu and Z. Wu, *Appl. Phys. Lett.*, 2013, **102**, 212411.
23 Y. Kokubun, K. Miura, F. Endo and S. Nakagomi, *Appl. Phys. Lett.*, 2007, **90**, 031912.
24 H. Hayashi, R. Huang, F. Oba, T. Hirayama and I. Tanaka, *J. Mater. Res.*, 2011, **26**, 578.
25 J. Okabayashi, A. Kimura, O. Rader, T. Mizokawa, A. Fujimori, T. Hayashi and M. Tanaka, *Phys. Rev. B: Condens. Matter Mater. Phys.*, 1998, **58**, R4211.
26 J. F. Moudler, W. F. Stickle, P. E. Sobol and K. D. Bomben, *Handbook of X-Ray Photoelectron Spectroscopy*, Perkin-Elmer, Eden Prairie, 1992.
27 B. Hu, B. Y. Man, C. Yang, M. Liu, C. S. Chen, X. G. Gao, S. C. Xu, C. C. Wang and Z. C Sun, *Appl. Surf. Sci.*, 2011, **258**, 525.
28 D. Y. Guo, Z. P. Wu, P. G. Li, Y. H. An, H. Liu, X. C. Guo, H. Yan, G. F. Wang, C. L. Sun, L. H. Li and W. H. Tang, *Opt. Mater. Express*, 2014, **4**, 1067.
29 T. Suzuki and T. Katsufuji, *Phys. Rev. B: Condens. Matter Mater. Phys.*, 2008, **77**, 220402.
30 G. Pei, C. Xia, Y. Dong, B. Wu, T. Wang and J. Xu, *Scr. Mater.*, 2008, **58**, 943.
31 N. Khare, M. J. Kappers, M. Wei, M. G. Blamire and J. L. MacManus-Driscoll, *Adv. Mater.*, 2006, **18**, 1449.
32 J. M. D. Coey, M. Venkatesan and C. B. Fitzgerald, *Nat. Mater.*, 2005, **4**, 173.
33 D. Loss and D. P. DiVincenzo, *Phys. Rev. A*, 1998, **57**, 120.
34 C. Song, K. Geng, F. Zeng, X. Wang, Y. Shen, F. Pan, Y. Xie, T. Liu, H. Zhou and Z. Fan, *Phys. Rev. B: Condens. Matter Mater. Phys.*, 2006, **73**, 024405.
35 S. Ogale, R. Choudhary, J. Buban, S. Lofland, S. Shinde, S. Kale, V. Kulkarni, J. Higgins, C. Lanci, J. Simpson, N. Browning, S. Das Sarma, H. Drew, R. Greene and T. Venkatesan, *Phys. Rev. Lett.*, 2003, **91**, 077205.